Interferometric Array Imaging

George Papanicolaou
Department of Mathematics, Stanford University
http://georgep.stanford.edu

In collaboration with:
L. Borcea (CAAM Rice) and **C. Tsogka** (Stanford Mathematics).

Imaging: Acquisition of the data

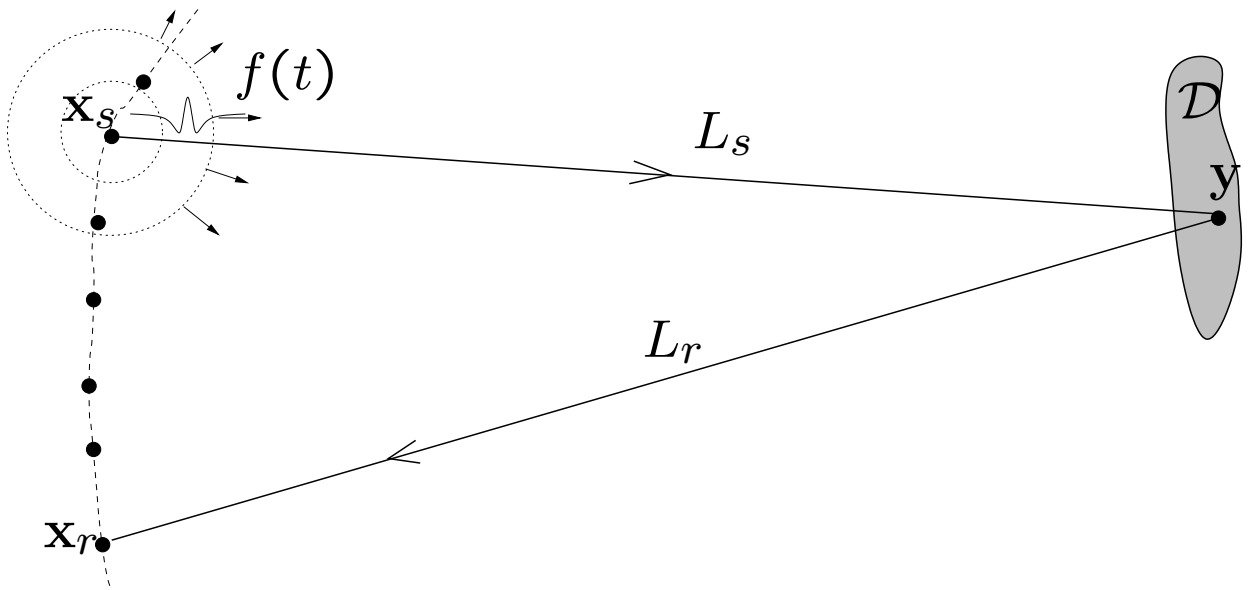

Active array data: $P(\mathbf{x}_s, \mathbf{x}_r, t)$ for $(\mathbf{x}_s, \mathbf{x}_r, t)$ a set of source-receiver locations in $R^2 \times R^2$ and time in R_+. A five-dimensional parametrization of the data. Passive: $P(\mathbf{x}_r, t)$, a three-dimensional dataset.

Different data acquisition geometries: Synthetic aperture imaging (zero-offset, large linear apertures, broadband), Ultrasonic imaging arrays (many sources and receivers, broadband signals).

Look carefully at resolution and noise issues.

Setup for numerical simulations I

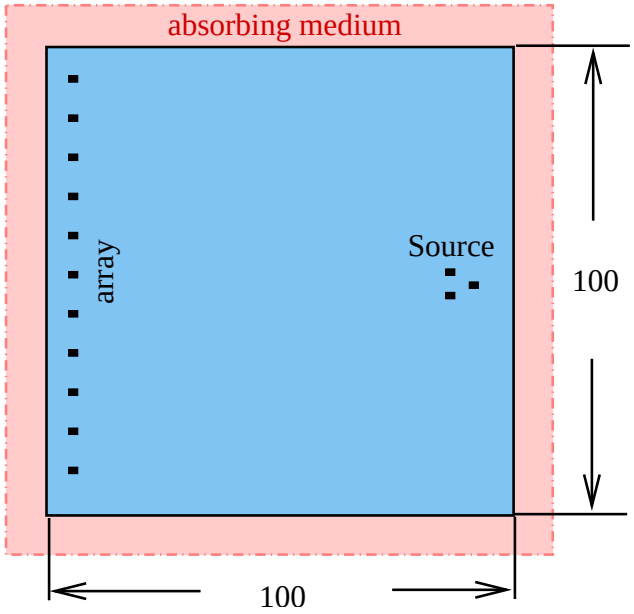

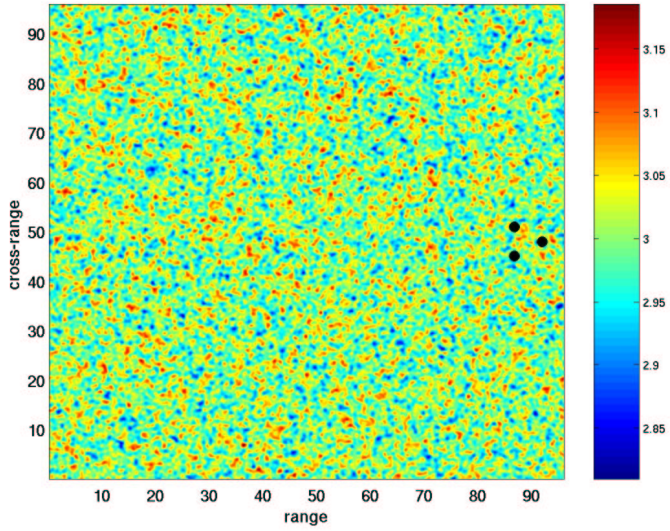

Computational domain $100\lambda_0 \times 100\lambda_0$ with central wavelength $\lambda_0 = 3m$ (at central frequency $f_0 = 1KHz$ and with $c_0 = 3km/sec$), surrounded by a perfectly matched layer (pink).

The array has 185 receiving elements $\lambda_0/2$ apart, for an aperture of $92\lambda_0$.

Setup for numerical simulations II

The three sources are ultrawideband (more than 100% bandwidth) at a distance of $90\lambda_0$ from the array. The near ones are $6\lambda_0$ apart and the far one is $3\lambda_0$ behind the near ones.

The random fluctuations of the propagation speed, on the right, have 3% STD and a Gaussian correlation (monoscale) function. The correlation length is equal to the central wavelength $\lambda_0 = 3m$.

We use a FINITE ELEMENT TIME DOMAIN CODE (2D or 3D), resolving all scales with $30 - 40$ points per wavelength. It takes about two hours on a workstation to produce a set of (2D) synthetic data.

We have well established 3D elastic and electromagnetic FETD codes. The codes are now being ported on a computer cluster that was obtained recently.

Passive array: traces

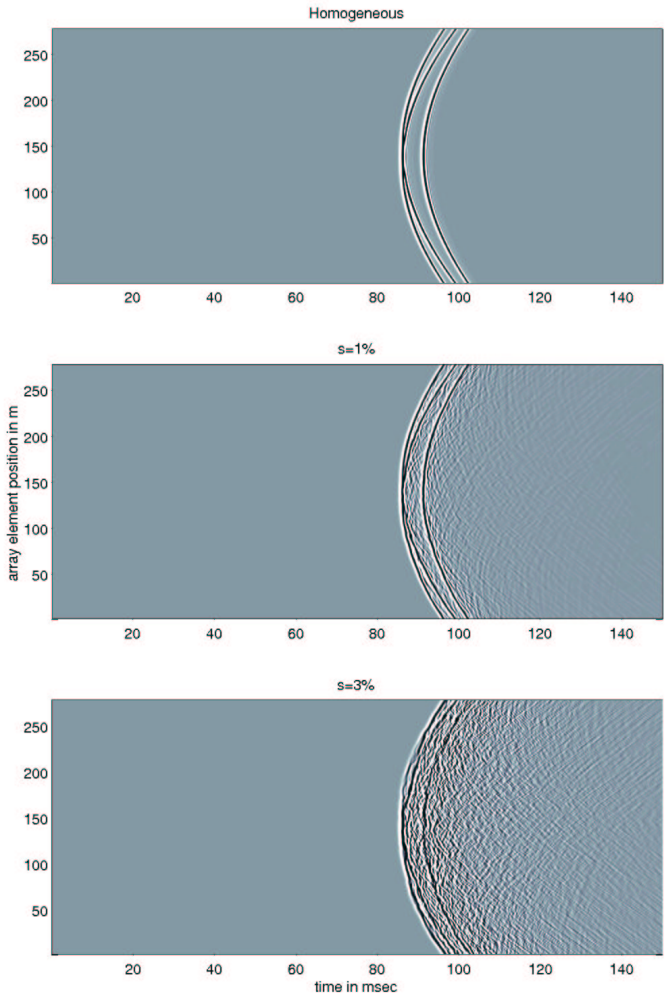

Down: Homogeneous, 1%, 3%STD.

Synthetic aperture imaging or Kirchhoff migration

The imaging functional for KM at a search point $\mathbf{y}^S$ is:

$$I^{KM}(\mathbf{y}^S) = \sum_r P(\mathbf{x}_r, \tau(\mathbf{x}_r, \mathbf{y}^S)) = \sum_r \frac{1}{2\pi} \int d\omega \widehat{P}(\mathbf{x}_r, \omega) e^{-i\omega\tau(\mathbf{x}_r, \mathbf{y}^S)}$$

where $\tau(\mathbf{x}, \mathbf{y}) = |\mathbf{x} - \mathbf{y}|/c_0$ is the travel time in a homogeneous background with propagation speed c_0.

It does not work well in clutter.

It is statistically unstable in clutter.

The reason is that KM tries to cancel (by back propagation or time reversal in a homogeneous medium) the random phase of the signals arriving at the array with a deterministic phase using travel times.

Kirchhoff migration imaging results

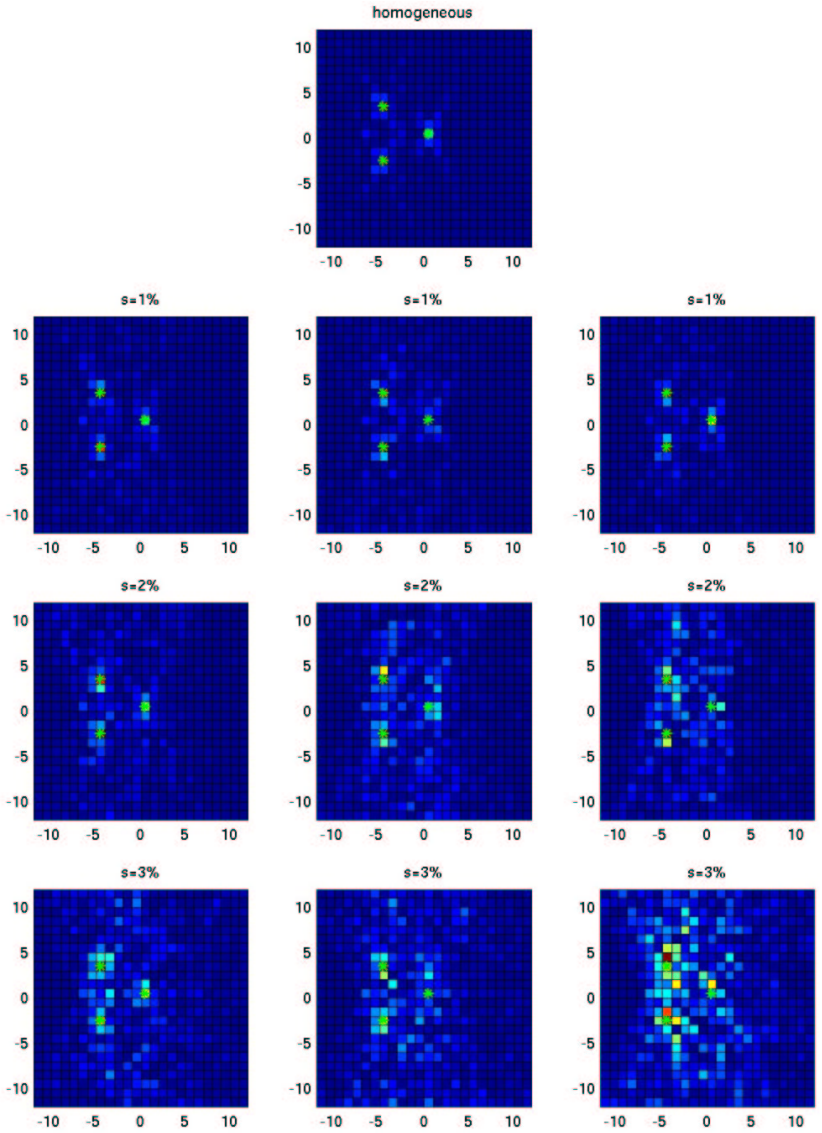

Down: Homogeneous, 1%, 2%, 3%STD. Across: different realizations.

Incoherent Interferometry

To avoid the random phase problems in Kirchhoff migration imaging we mimic time reversal by computing cross-correlations of data traces, the interferograms, and summing

$$I^{INT}(\mathbf{y}^S) = \sum_{\mathbf{x}_r, \mathbf{x}_{r'}} P(\mathbf{x}_r, \cdot) *_t P(\mathbf{x}_{r'}, -\cdot)|_{\tau(\mathbf{x}_r, \mathbf{y}^S) - \tau(\mathbf{x}_{r'}, \mathbf{y}^S)}$$

The interferograms are self-averaging. We are doing Differential Kirchhoff Migration on the lag of the interferograms.

In the frequency domain we have

$$I^{INT}(\mathbf{y}^S) = \int d\omega \left| \sum_{\mathbf{x}_r} \widehat{P}(\mathbf{x}_r, \omega) e^{-i\omega\tau(\mathbf{x}_r, \mathbf{y}^S)} \right|^2$$

But this is almost Matched Field Imaging

$$I^{MF}(\mathbf{y}^S) = \int d\omega \left| \sum_{\mathbf{x}_r} \overline{\widehat{P}(\mathbf{x}_r, \omega)} \widehat{G}_0(\mathbf{x}_r, \mathbf{y}^S, \omega) \right|^2, \quad \widehat{G}_0(\mathbf{x}, \mathbf{y}, \omega) = \frac{e^{i\omega\tau(\mathbf{x}, \mathbf{y})}}{4\pi|\mathbf{x} - \mathbf{y}|}$$

Time reversal interpretation

The interferograms

$$P(\mathbf{x}_r, \cdot) *_t P(\mathbf{x}_{r'}, -\cdot)(t) = \int_{-\infty}^{\infty} P(\mathbf{x}_r, s) P(\mathbf{x}_{r'}, s - t) ds$$

have a time reversal interpretation (based on the reciprocity of Green's functions):

A signal is emitted from $\mathbf{x}_{r'}$ and is recorded at the (unknown) source location $\mathbf{y}$. The recorded signal is time-reversed and re-emitted into the medium. The signal received at $\mathbf{x}_r$ is the interferogram above.

The interferogram decorrelates rapidly in a random medium as the distance between $\mathbf{x}_r$ and $\mathbf{x}_{r'}$ increases.

The decorrelation distance Δ_d is related to the effective aperture in time reversal, which is essentially independent of any physical aperture. It can be ESTIMATED from the array data directly.

Time reversal basics

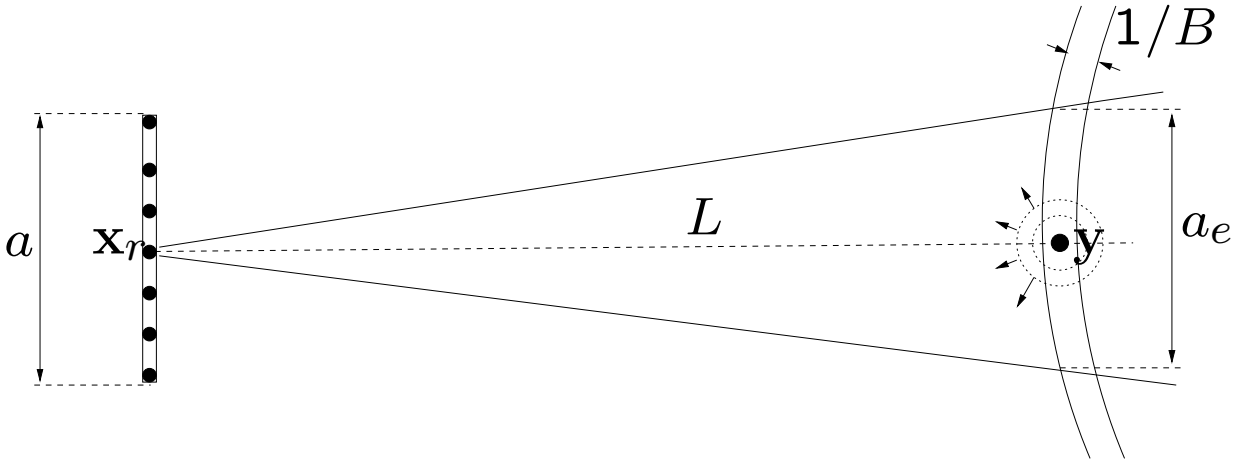

A source at $\mathbf{y}$ emits a pulse received at $\mathbf{x}_r$. Recorded data is:

$$\widehat{P}(\mathbf{x}_r, \omega) = \widehat{f}_B(\omega - \omega_0)\widehat{G}(\mathbf{x}_r, \mathbf{y}, \omega)$$

If we knew the Greens's function (travel time) of the medium then we image or do real time reversal (or back propagation) with

$$\Gamma^{TR}(\mathbf{y}^S) = \int d\omega \sum_{\mathbf{x}_r} \overline{\widehat{P}(\mathbf{x}_r, \omega)}\widehat{G}(\mathbf{x}_r, \mathbf{y}^s, \omega)$$

In TIME REVERSALthe spot size around the source location is $\frac{\lambda_0 L}{a_e}$, with $a_e >> a$ the effective aperture. Super-resolution.

Focusing in (real) time reversal

Interferometric imaging is motivated by the fact that focusing in real time reversal improves when there is clutter (super resolution), in a statistically stable way. There is, however, loss of energy, again because of the clutter.

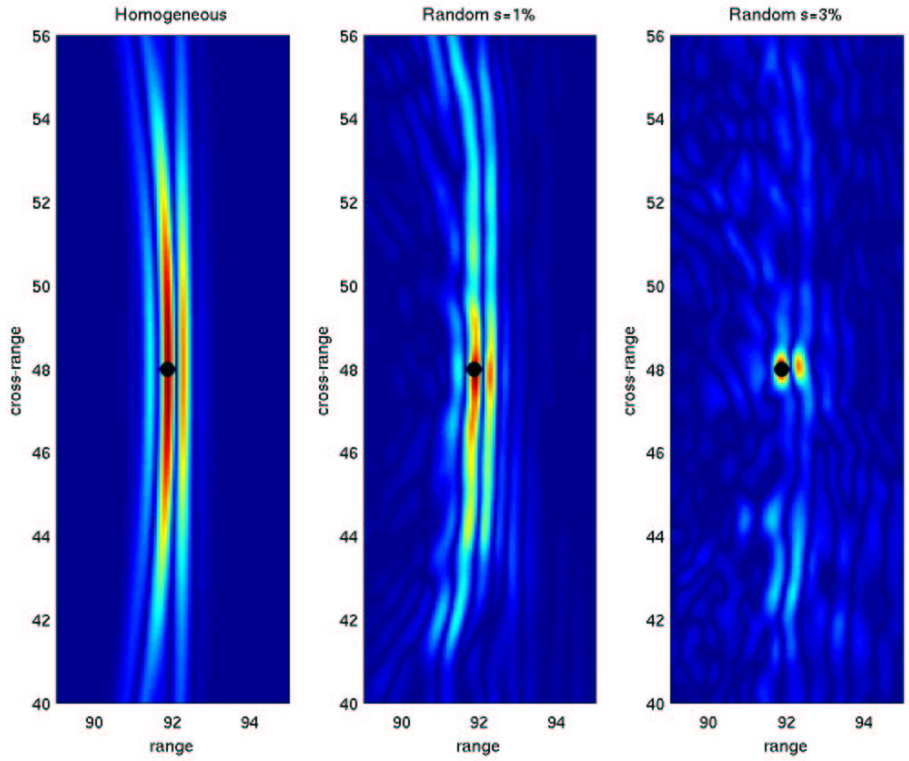

Across: Homogeneous, 1%, 3%STD, for an array of size $10\lambda_0$. The focusing strength is normalized to have peak equal to one.

Limitations of incoherent interferometry

- Incoherent interferometric imaging is effective only if the decoherence frequency Ω_d is very small, essentially zero relative to the bandwidth. Frequency coherence is not used!

- Incoherent interferometric imaging gets depth resolution only by triangulation, which needs large arrays. Sometimes an arrival time analysis can give depth resolution but there is no robust way to do this.

- Incoherent interferometry gets direction of arrival (angular) resolution from which the decoherence length Δ_d can be ESTIMATED. Broadband is essential here (Inverse Problems, vol 19, (2003), pp. 5139-5164).

To combine good random phase cancellation, which KM does not have but INT and MF have, with exploitation of residual coherence effects we introduce the Coherent Interferometric functional:

$$I^{CINT}(\mathbf{y}^S) = \int\int_{|\omega_1-\omega_2|\leq\Omega_d} d\omega_1 d\omega_2 \sum\sum_{|\mathbf{x}_r-\mathbf{x}'_r|\leq\Delta_d} \widehat{P}(\mathbf{x}_r,\omega_1)\overline{\widehat{P}(\mathbf{x}'_r,\omega_2)}e^{-i(\omega_1\tau(\mathbf{x}_r,\mathbf{y}^S)-\omega_2\tau(\mathbf{x}'_r,\mathbf{y}^S))}$$

Using midpoint (sum) and offset (difference) variables: $\mathbf{x}_r = \bar{\mathbf{x}}-\tilde{\mathbf{x}}/2,\ \mathbf{x}'_r = \bar{\mathbf{x}}+\tilde{\mathbf{x}}/2$ and $\omega_1 = \bar{\omega}-\tilde{\omega}/2,\ \omega_1 = \bar{\omega}+\tilde{\omega}/2$ we rewrite it as

$$I^{CINT}(\mathbf{y}^S) = \int d\bar{\omega} \sum_{\bar{\mathbf{x}}} \int_{|\tilde{\omega}|\leq\Omega_d} \sum_{|\tilde{\mathbf{x}}|\leq\Delta_d} \widehat{P}(\bar{\mathbf{x}}-\frac{\tilde{\mathbf{x}}}{2},\bar{\omega}-\frac{\tilde{\omega}}{2})\overline{\widehat{P}(\bar{\mathbf{x}}+\frac{\tilde{\mathbf{x}}}{2},\bar{\omega}+\frac{\tilde{\omega}}{2})} e^{i\bar{\omega}[\tau(\bar{\mathbf{x}}+\frac{\tilde{\mathbf{x}}}{2},\mathbf{y}^S)-\tau(\bar{\mathbf{x}}-\frac{\tilde{\mathbf{x}}}{2},\mathbf{y}^S)]}e^{\frac{i\tilde{\omega}}{2}[\tau(\bar{\mathbf{x}}-\frac{\tilde{\mathbf{x}}}{2},\mathbf{y}^S)+\tau(\bar{\mathbf{x}}+\frac{\tilde{\mathbf{x}}}{2},\mathbf{y}^S)]}$$

Wigner function of the data

Using the space-wavenumber, time-frequency Wigner function of the data

$$W_D(\bar{\mathbf{x}}, \mathbf{p}; \bar{t}, \bar{\omega}) = \int_{|\tilde{\omega}| \leq \Omega_d} d\tilde{\omega} \sum_{|\tilde{\mathbf{x}}| \leq \Delta_d} \widehat{P}(\bar{\mathbf{x}} - \frac{\tilde{\mathbf{x}}}{2}, \bar{\omega} - \frac{\tilde{\omega}}{2}) \overline{\widehat{P}(\bar{\mathbf{x}} + \frac{\tilde{\mathbf{x}}}{2}, \bar{\omega} + \frac{\tilde{\omega}}{2})} e^{i(\mathbf{p} \cdot \tilde{\mathbf{x}} + \bar{t}\tilde{\omega})}$$

and simplifying, the **coherent interferometric functional** is

$$I^{CINT}(\mathbf{y}^S) = \int d\bar{\omega} \sum_{\bar{\mathbf{x}}} W_D(\bar{\mathbf{x}},\ \bar{\omega} \nabla_{\bar{\mathbf{x}}} \tau(\bar{\mathbf{x}}, \mathbf{y}^S);\ \tau(\bar{\mathbf{x}}, \mathbf{y}^S),\ \bar{\omega})$$

This is the imaging functional that we use in the results shown next, where we also vary the decoherence frequency Ω_d and the decoherence distance Δ_d.

Coherent interferometric imaging results I

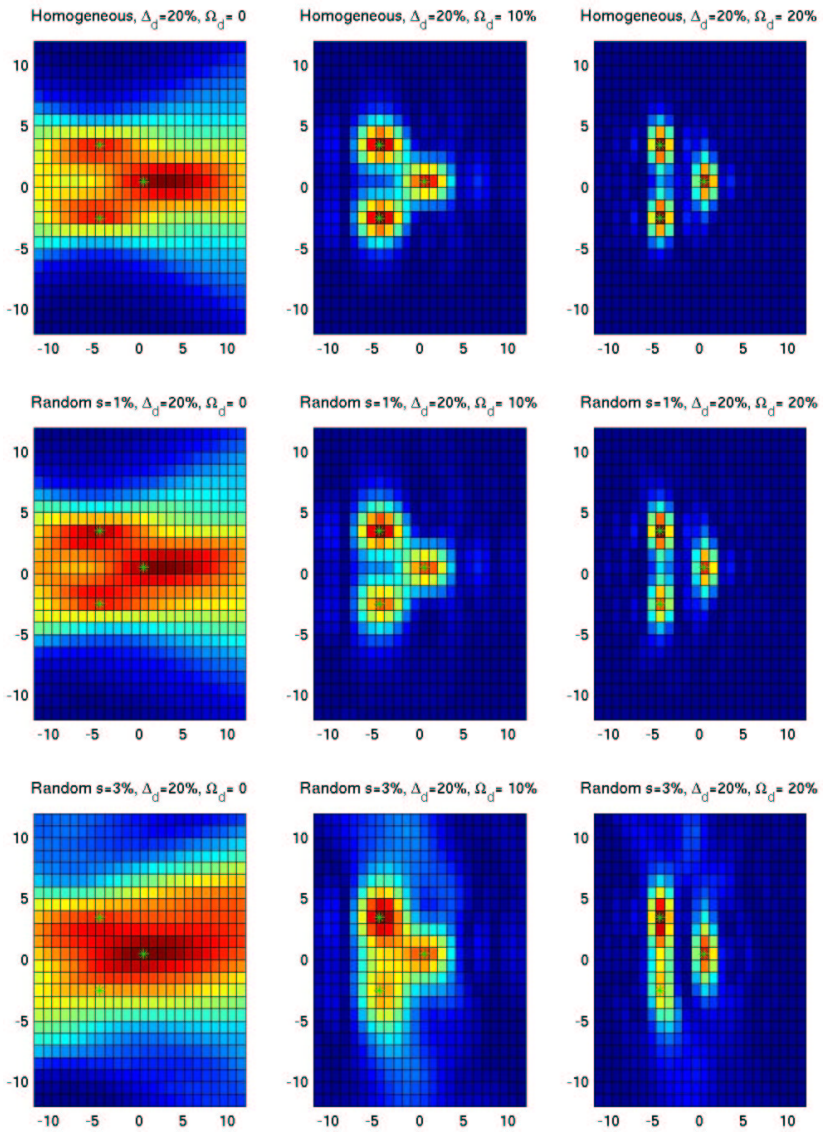

Down: 0%, 1%, 3% STD. Across: $\Omega_d = 0, 10, 20\%$. All: $\Delta_d = 20\%$

Coherent interferometric imaging results II

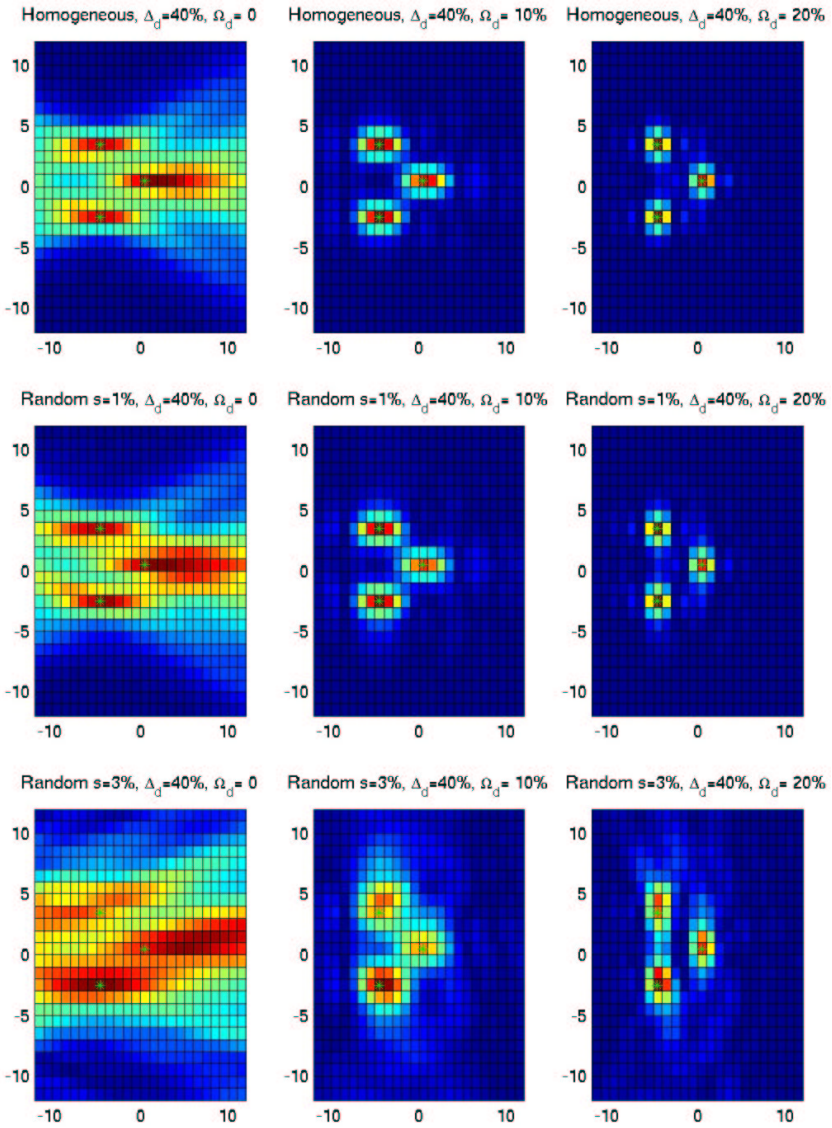

Down: 0%, 1%, 3% STD. Across: $\Omega_d = 0, 10, 20\%$. All: $\Delta_d = 40\%$

Coherent interferometric imaging results III

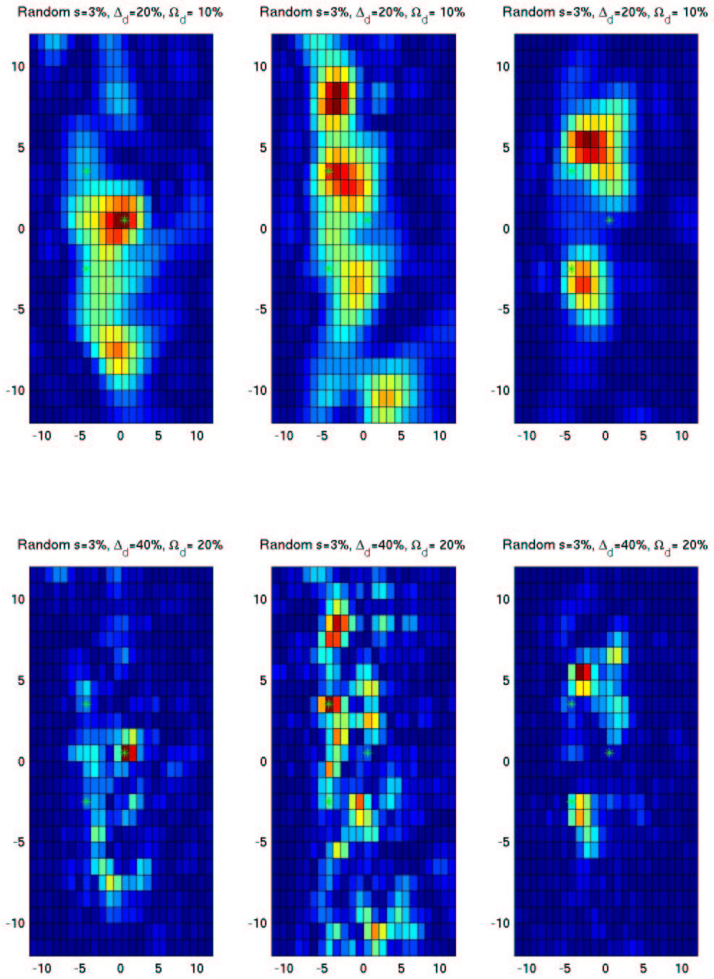

No $\bar{\omega}$ averaging. Three realizations at 3% STD. Top: $\Omega_d = 10\%$ $\Delta_d = 20\%$. Bottom: $\Omega_d = 10\%$ $\Delta_d = 40\%$. No statistical stability when bandwidth is not used fully.

Coherent interferometric imaging results IV

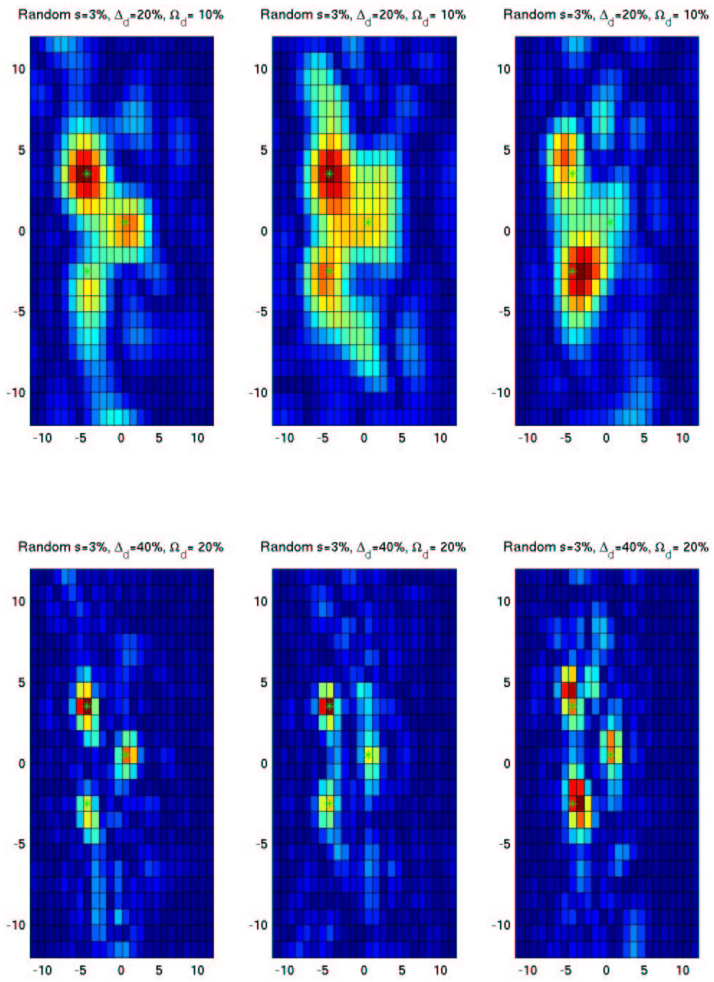

Sum of three $\bar{\mathbf{x}}$'s. Three realizations at 3% STD. Top: $\Omega_d = 10\%$ $\Delta_d = 20\%$. Bottom: $\Omega_d = 10\%$ $\Delta_d = 40\%$. Some statistical stability when array is not used fully.

Resolution theory

A resolution theory can be developed based on several assumptions about the random medium and the propagation regime.

- With the paraxial approximation, the white noise limit, and a high frequency expansion we reduce all theoretical calculations to the use of one relatively simple formula obtained from the random Schrödinger equation

- The main results are: (a) the resolution in range is c_0/Ω_d with c_0 the homogeneous propagation speed, and (b) the angular or direction of arrival resolution is $(k_0\Delta_d)^{-1}$ with k_0 the central wavenumber. We assume here that the SNR at the array is high (essentially infinite)

Active array or echo-mode imaging

In the echo-mode numerical simulations we use a configuration of three (Dirichlet) scatterers of size equal to one central wavelength λ_0, at the same location as the sources in the passive mode simulations.

Three array elements act as sources of illumination, one at a time: one central and two side elements.

We show calculations with 1% STD of fluctuations. In echo-mode the random medium is, however, twice as long as in direct mode imaging so its effect is stronger.

We use the coherent interferometric imaging functional $I^{CINT}(\mathbf{y}^S)$ for each illumination.

Active array imaging schematic

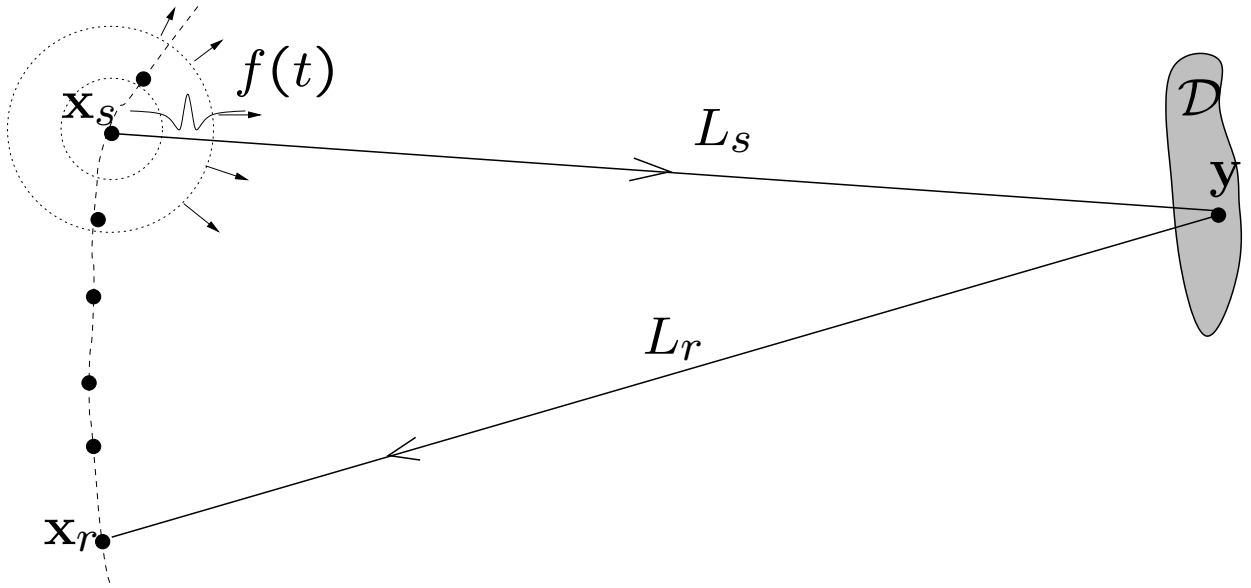

Array data: $P(\mathbf{x}_s, \mathbf{x}_r, t)$ for $(\mathbf{x}_s, \mathbf{x}_r, t)$ a set of source-receiver locations in $R^2 \times R^2$ and time in R_+. Up to a five-dimensional parametrization of the data is possible.

In the numerical simulations we use only three source locations $\mathbf{x}_s$, one at a time.

Active array or echo-mode imaging: traces

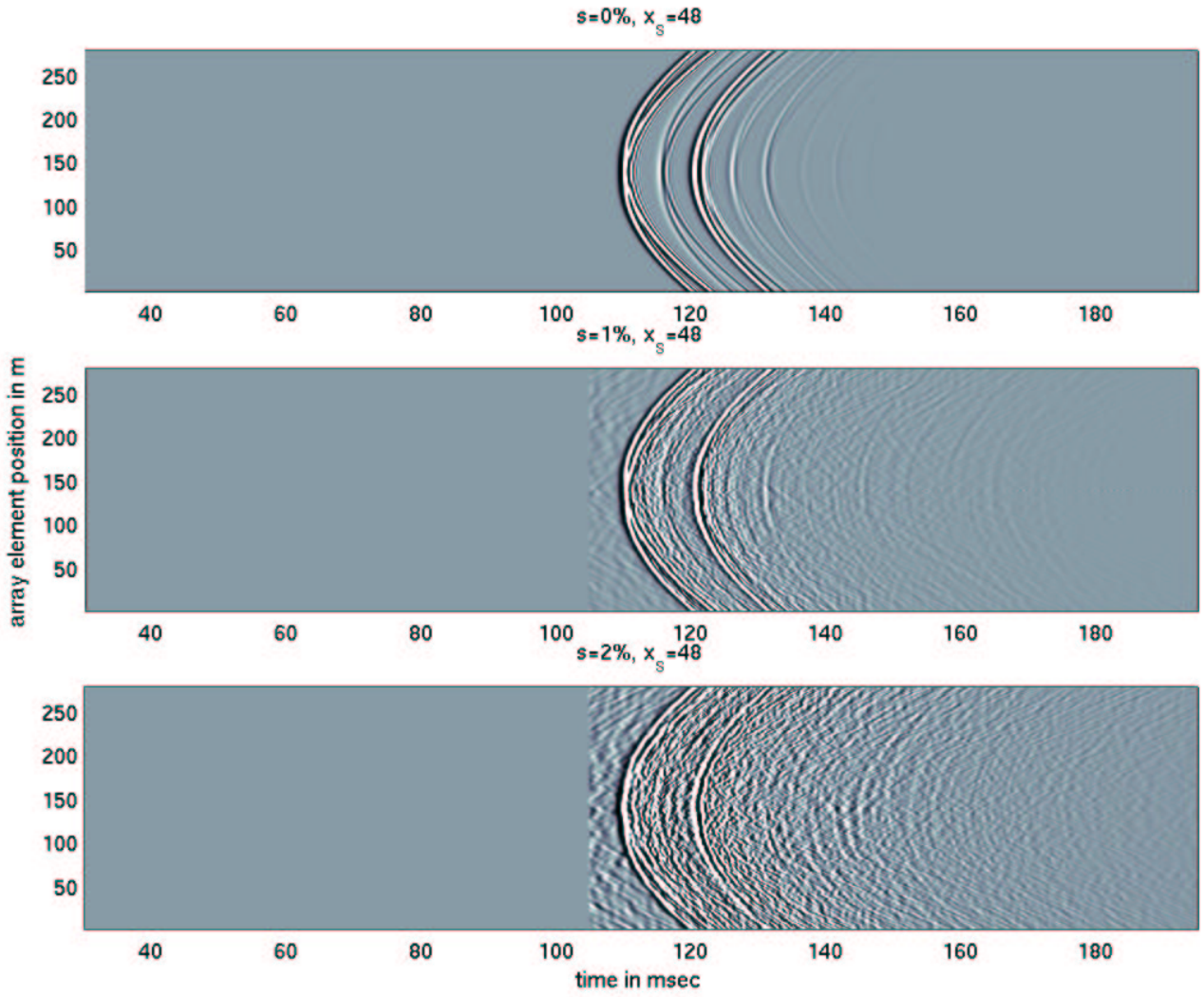

Down: homogeneous, $s = 1\%$ and 2% STD.

Active or echo-mode imaging results I

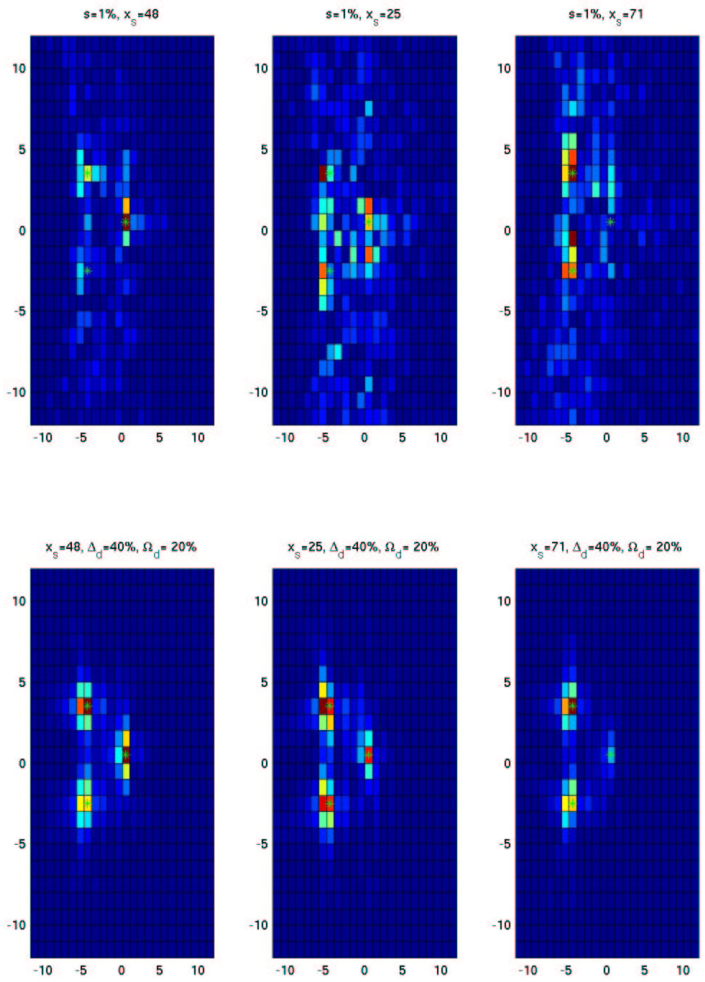

Across: central, right side, left side illumination. Top: Kirchhoff migration with 1% STD. Bottom: Coherent interferometry with 1% STD, $\Omega_d = 20\%$ and $\Delta_d = 40\%$.

Active or echo-mode imaging results II

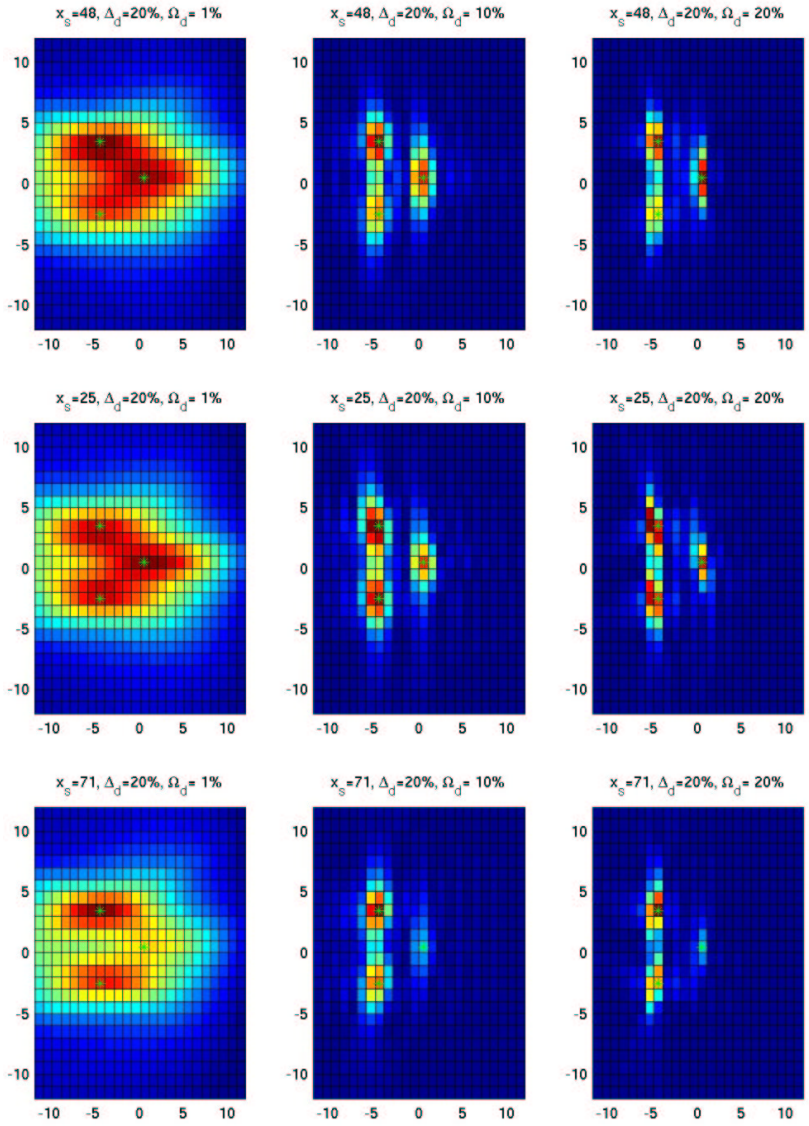

Down: $\mathbf{x}_s =$ center, right and left. Across: $\Omega_d = 1\%,\ 10\%,\ 20\%$; $\Delta_d = 20\%$.

Active or echo-mode imaging results III

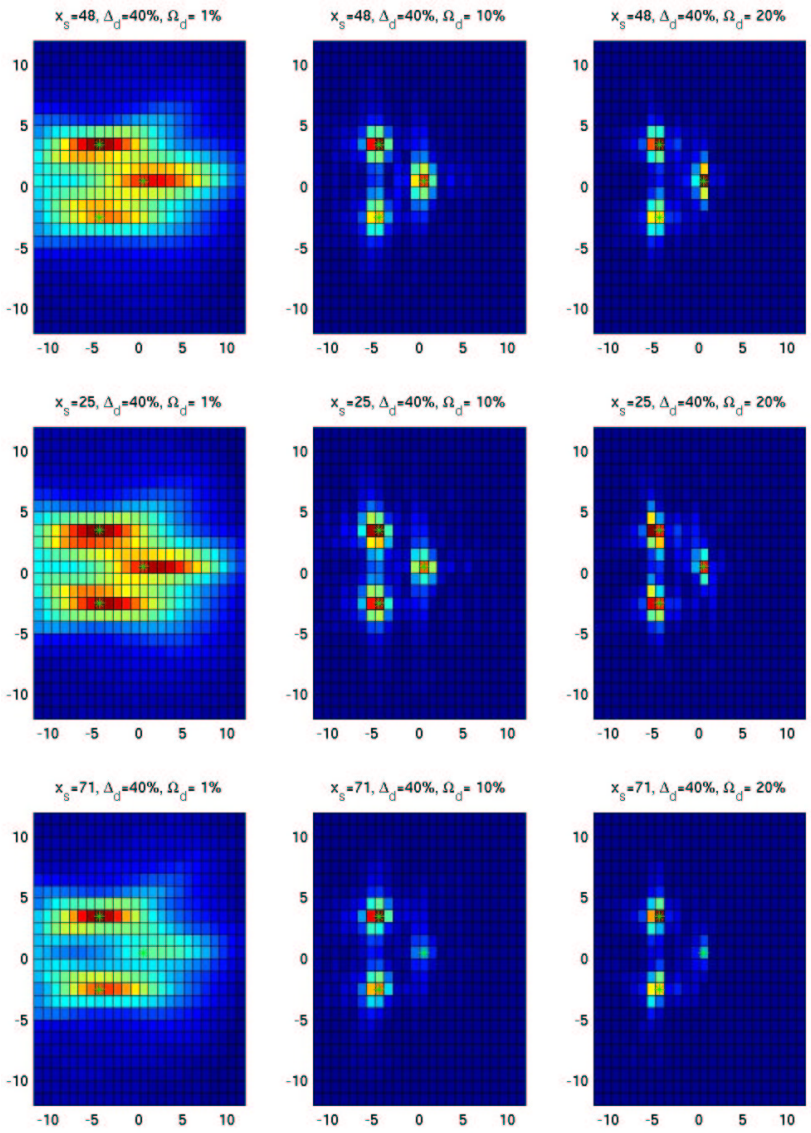

Down: $\mathbf{x}_s =$ center, right and left. Across: $\Omega_d = 1\%,\ 10\%,\ 20\%$; $\Delta_d = 40\%$.

Active or echo-mode imaging results IV

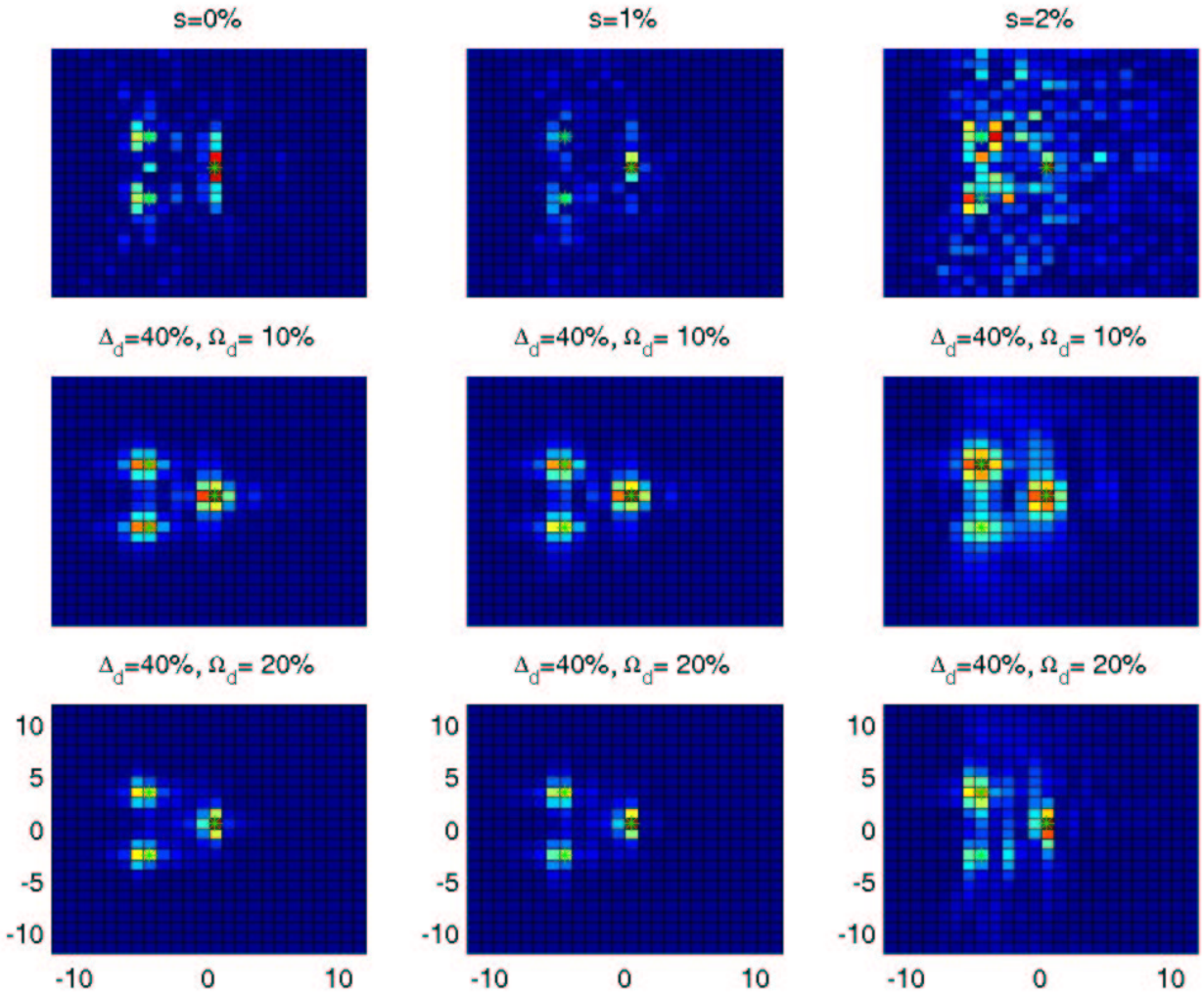

Center illumination. Top row is Kirchoff Migration.

Concluding remarks

- Coherent interferometry, which is the backpropagation of local cross-correlations of traces, is a very effective way to deal with cluttered environments in array imaging and remote sensing.

- Coherent interferometry uses the good properties of time reversal in random media (super-resolution and statistical stability in the time domain) optimally.